Dielectric and Viscoelastic Studies of Segmental and Normal Mode Relaxations in Undiluted Poly(*d*,*l*-lactic acid)

Jindong Ren, Osamu Urakawa, and Keiichiro Adachi*

Department of Macromolecular Science, Graduate School of Science, Osaka University, Toyonaka, Osaka 560-0043, Japan

Received July 30, 2002; Revised Manuscript Received November 4, 2002

ABSTRACT: We report the dielectric and viscoelastic relaxations in undiluted amorphous poly(*d*,*l*-lactic acid) (PLA). Three dielectric relaxations designated as α_n, α_s, and β are observed in order of decreasing temperature. The relaxation time for the α_n relaxation increases with increasing molecular weight and is assigned to the normal mode relaxation due to the component of dipole vector aligned in the direction parallel to the chain contour. The α_s relaxation is observed about 30 K above the glass transition temperature T_g (= 310 K) and is assigned to the local segmental mode due to the transverse component of the monomeric dipoles. The β relaxation is seen in the glassy state and is assigned to the secondary relaxation. From the relaxation strengths for the α_n, α_s, and β relaxations, the effective dipole moments for those relaxation processes are determined and compared with the parallel and transverse components of the dipole moment calculated theoretically with the semiempirical molecular orbital methods. The dielectric relaxation time for the normal mode increases with molecular weight M with the power of 3.5 in the range of molecular weight above the characteristic molecular weight M_c (= 13 000). The molecular weight between entanglements is calculated to be 7700 from the shear modulus in the rubbery plateau region. It is found that the dielectric normal mode relaxation time agrees approximately with the viscoelastic terminal relaxation time. The relaxation spectra for the viscoelastic relaxation are much broader than those for the dielectric relaxation as observed previously for polyisoprene.

Introduction

Polymers having dipoles aligned in the direction parallel to the chain contour are classified by Stockmayer[1] as type A and exhibit the *dielectric normal mode relaxation* due to fluctuation of the end-to-end vector.[2−4] The dielectric spectroscopy on the normal mode relaxation provides fruitful information on global chain dynamics.[1,2] Aliphatic polyesters having structures given by $-(R_m-COO)_n-$ are one of type-A polymers where R_m represents an aliphatic hydrocarbon composed of m backbone atoms. Jones et al.[5] first reported the dielectric normal mode relaxation in dilute solutions of poly(ϵ-caprolactone) (m = 5). Later Urakawa et al.[6] reported the dielectric normal mode relaxations in solutions of poly(ϵ-caprolactone) and poly(varelo lactone) (m = 4) with a narrow distribution of molecular weight. The dielectric normal mode relaxation of undiluted polymers was extensively studied for polyisoprene,[7−10] but that of undiluted polyesters has not been reported.

Poly(lactic acid) (PLA) is an aliphatic polyester of m = 1 as shown in Figure 1a where C_4 is the carbon atom of the next repeat unit. Because of the resonance effect, the C_2-O_3 bond has a character of double bond and hence the internal rotation around C_2-O_3 occurs hardly.[11] Therefore, the backbone atoms C_1, C_2, O_3, and C_4 are on a same plane, and hence, the whole repeat unit can be regarded as a virtual bond (dashed line in Figure 1) as pointed out by Jones et al.[5] The virtual bond possesses the parallel (type A) and transverse (type B) components of the dipole moment p_A and p_B (Figure 1). Thus, PLA is expected to exhibit the normal mode relaxation.

The type-B dipoles cause the dielectric relaxation due to local segmental motions. The type-B dipole vector $\mathbf{p}_B$ reorients through internal rotation with respect to the C_1-C_2 and O_3-C_4 bonds. The spatial correlation between the type-B dipoles results in cooperative motions of the segments. The mechanism of segmental motion is long lasting issue and has not been clarified perfectly. We will examine the cooperative nature of the type-B dipoles of the PLA molecule based on the observed effective dipole moment.

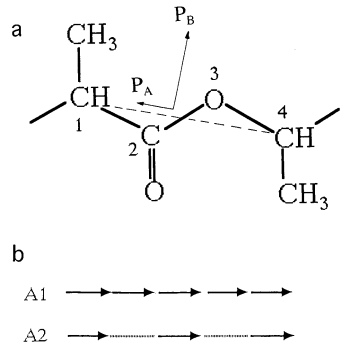

Figure 1. (a) Chemical structure of the monomeric unit of PLA and the parallel (p_A) and transverse (p_B) dipole vectors. The dashed line indicates the virtual bond. (b) Classification of type-A polymers. In a type-A1 polymer, the whole monomeric unit is rigid and can be regarded as a virtual bond. In a type-A2 polymer, the monomeric unit is formed from the polar and nonpolar units.

For undiluted polyisoprene,[7−10] it has been revealed that the relaxation time τ_n for the normal mode depends strongly on molecular weight M: $\tau_n \propto M^{3.7}$ in the range of $M > M_c$ and in the range $M < M_c$, $\tau_n \propto M^{2.0}$. Here M_c denotes the characteristic molecular weight. So far the dielectric normal mode relaxation in the entangled regime has been studied only for polyisoprene although dielectric relaxations of several type-A polymers were studied in the solution state[4] or in the nonentangled

* Corresponding author.

10.1021/ma0212341 CCC: $25.00
Published on Web 12/12/2002

regime.[12−15] Additional dielectric data of undiluted type-A polymers are required for understanding the general behavior of entangled polymers.

Depending on the configuration of the type-A dipoles on chains, type-A polymers can be classified further into types A1 and A2 as shown schematically in Figure 1b.[6] In type-A1 polymers, the parallel dipoles are connected directly, but in type-A2 polymers, the dipoles are connected with nonpolar groups. In dynamical processes of a type-A1 chain, its overall dipole moment is exactly proportional to the end-to-end vector, but for type-A2 polymers, this does not hold. The whole monomeric unit of PLA can be regarded as a virtual bond, and therefore, PLA is a type-A1 polymer. A few type-A1 polymers are known, i.e., poly(2,6-dichlorophenylene oxide),[16] poly(butyl acetylene),[17] and poly(phenoxy phosphazene).[18] Although the dielectric normal mode relaxations in solutions of those polymers have been reported, no dielectric studies on undiluted type-A1 polymers have been reported.

The dielectric normal mode relaxation is closely related to the terminal viscoelastic relaxation. We studied the relationship between the dielectric and viscoelastic relaxations. Comparison of the dielectric and viscoelastic relaxations have been also made for undiluted polyisoprene.[19] It was found that the relaxation time for the dielectric normal mode coincides approximately with the terminal viscoelastic relaxation. However, the relaxation spectrum for the viscoelastic relaxation is much broader than that for the dielectric normal mode. We will examine whether PLA also exhibits such behavior.

So far no dielectric studies have been reported on perfectly amorphous polyesters. Yager and Baker[20] reported the dielectric and mechanical relaxations in polyesters having structure of $(-O-CO-R_s-CO-O-R_m-)_n$ where *s* and *m* denote the number of methylene groups. Wurstlin[21] also studied the dielectric relaxation in linear polyesters of this type. Those polyesters are crystalline polymers and do not possess type-A dipoles since the parallel dipoles of the two ester groups of the repeat unit cancel each other. Viscoelastic relaxation of *l*-PLA was reported by Justin and Michael.[22]

Aliphatic polyesters are biodegradable. Thus, PLA has been investigated as a potential engineering material[23,24] and is used as a nontoxic, naturally occurring, and renewable material. Commercial PLAs are usually *d*- or *l*-PLAs and are crystalline polymers. The biodegradability, biocompatibility, and mechanical properties of those PLA have been also extensively studied for their potential uses in the biomedical field.[25] On the other hand, random copolymers of *d*- and *l*-lactides are amorphous. However, studies on amorphous PLA are relatively rare.

In view of the background mentioned above, we have carried out dielectric and viscoelastic measurements on amorphous PLAs. In this paper, we first report the overall dielectric relaxation behavior of amorphous PLA. Then we will discuss the dipole moment and the internal field factor for the normal mode relaxation. Finally we compare the dielectric normal mode relaxation and viscoelastic relaxations.

Experimental Section

Materials. Two kinds of *d*,*l*-PLA samples were used. One group of the samples is perfectly racemic PLA purchased from Wako Chemicals (Tokyo, Japan) and is denoted as S0. We also prepared *d*,*l*-PLA by copolymerization of a 1:1 mixture of *l*- and *d*,*l*-dilactides with a small amount of catalysts Sn-$(C_8H_{15}O_2)_2$ and dodecanol as described by Ajioka et al.[26] The monomers *l*-dilactide and *d*,*l*-dilactictide were purchased from Aldrich (SanFrancisco CA) and used as received. The catalysts were obtained from Wako Chemicals (Tokyo, Japan). The mixture was dried in a vacuum of 0.1 Pa overnight and then heated to 170−200 °C under atmosphere of dry helium. Above the melting point of the dilactide, the mixture was stirred. Changing the amount of the catalysts from 0.01 to 1 wt %, we obtained four original samples S1−S4 of different average molecular weight. Those samples were fractionated with dioxane as a good solvent and methanol or *n*-hexane as nonsolvents. The molecular weights of those fractions were measured with size exclusion chromatography by using an apparatus equipped with a low-angle laser-light scattering detector (Tosoh, Tokyo, Japan). Results are summarized in Table 1. The density of undiluted *d*,*l*-PLA was measured to be 1.246 g/mL (298 K) by a vuoyancy method.

Table 1. Characteristics of the PLA Samples

group	code	$10^{-3}M_w$	M_w/M_n	T_g	*d*/*l* ratio
S0	PLA-15	15.3	1.15	304	5/5
	PLA-27	26.8	1.20	304	5/5
	PLA-47	47.1	1.33	304	5/5
S1	PLA-75	75.3	1.17		1/3
	PLA-38	37.9	1.22		1/3
	PLA-29	28.5	1.17		1/3
	PLA-21	20.7	1.21		1/3
	PLA-12	11.7	1.21		1/3
S2	PLA-8	8.4	1.21	313	1/3
	PLA-5	4.8	1.23	307	1/3
	PLA-3	3.8	1.20		1/3
S3	PLA-16	16.4	1.26		1/3
	PLA-13	13.2	1.20		1/3
	PLA-11	10.5	1.21		1/3
	PLA-9	9.0	1.19		1/3
	PLA-7	6.8	1.22		1/3
	PLA-4	4.0	1.28		1/3
S4	PLA-119	1190	1.19		1/3
	PLA-86	85.7	1.11		1/3
	PLA-48	48.0	1.19		1/3

Methods. Dielectric measurements were carried out with RLC bridges (QuadTech models 7600 and 1693, Maynard) over the frequency range from 10 Hz to 2 MHz and temperature range from 80 to 430 K. The condenser cell for dielectric measurements of viscous liquids was reported previously.[9] The condenser was composed of guarded and unguarded electrodes. The unguarded electrode had a shape of a vessel with flat bottom. A piece of glassy PLA sample was put on the unguarded electrode and was kept in a vacuum at 370 K until bubbles disappeared. Then the sample was sandwiched between the guarded and unguarded electrodes at 370 K in a vacuum oven.

Dynamic shear moduli were measured with a dynamic stress rheometer (Rheometrics SR-200, Piscataway, NJ). Measurements were made with parallel plates of the diameter of 25 mm at the stress of 50 Pa and in the range of angular frequency from 0.5 to 500 rad/s. Measurements were carried out in the linear region.

Differential scanning calorimetry (DSC) was conducted at the heating rate of 10 K/min by using an apparatus (Seiko SSC-580, Tokyo, Japan). The glass transition temperature (T_g) was defined as the middle point of the stepwise change of the baseline. No melting peak was detected around the melting point of *l*-PLA (=430 K).

The optical rotatory power was measured with a spectropolarimeter (JASCO, J-720WO, Tokyo, Japan).

Results and Discussion

Multiple Dielectric Relaxation Behavior. Representative temperature dependence curves of the dielectric constant ϵ' and loss factor ϵ'' for PLA-8(1/3) and PLA-27(5/5) are shown in Figures 2 and 3, respectively. As described above, the ratio of *d*- and *l*-units of PLA-8

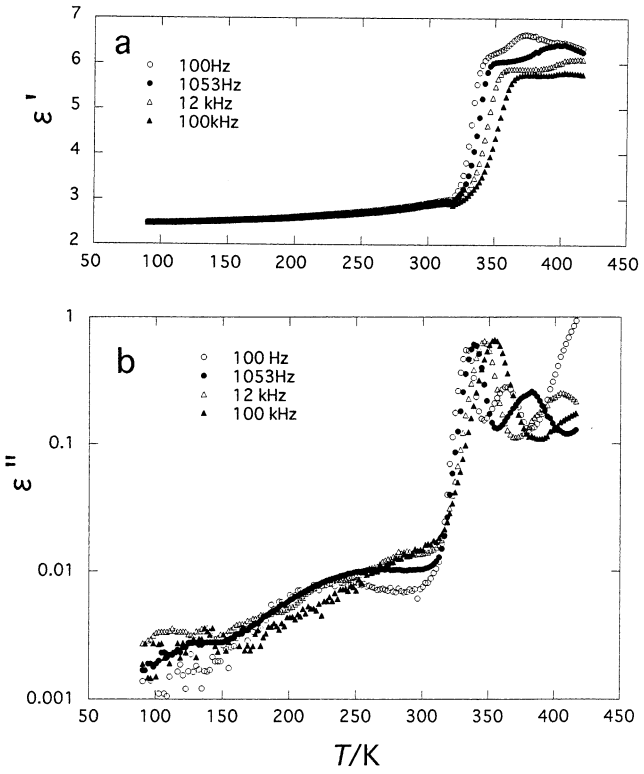

Figure 2. Temperature dependencies of the dielectric constant ϵ' (a) and loss factor ϵ'' (b) for PLA-8(1/3) at frequencies indicated in this figure.

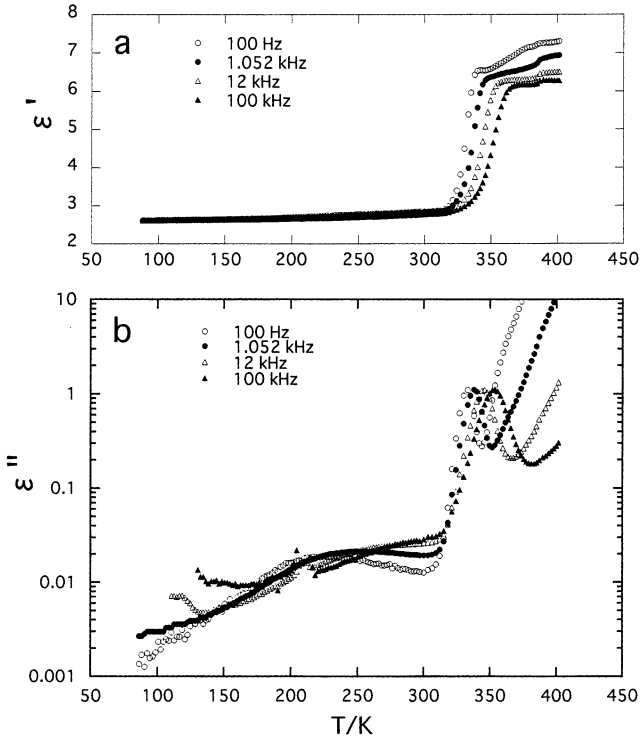

Figure 3. Temperature dependencies of the dielectric constant ϵ' (a) and loss factor ϵ'' (b) for PLA-27(5/5) at frequencies indicated in this figure.

is 1/3 and that of PLA-27 is 5/5. In this section we indicate the *d*/*l* ratios of the samples with the codes (1/3) and (5/5). In later sections we will abbreviate these codes. In the ϵ'' curves for PLA-8(1/3) we see three loss peaks designated as α_n, α_s, and β at about 380, 345, and 240 K, respectively, at 1 kHz. Corresponding to the ϵ'' peaks for the α_n and α_s relaxations, the ϵ' curve exhibits dispersions. Above 400 K, the ϵ'' curve at 100 Hz increases steeply with temperature on account of ionic conduction. In Figure 3, we see that the effect of the ionic conduction is stronger than that seen in Figure 2. The loss peak due to the α_n relaxation is not seen because of the ionic conduction. However the ϵ' curves exhibit clearly the small dispersion due to the α_n relaxation around 360 K.

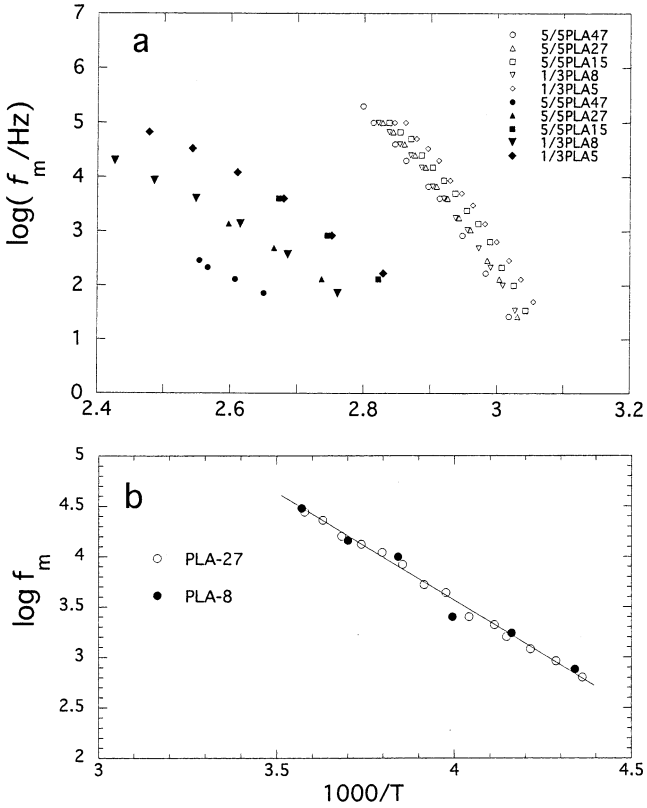

Figure 4. Arrhenius plots of the loss maximum frequencies f_m for the normal and segmental modes for representative PLA samples indixated in the figure (a) and those for the β relaxation (b).

The loss maximum frequencies f_m for the α_n relaxations (f_{mn}) and those for the α_s relaxations (f_{ms}) are plotted against the inverse of temperature in Figure 4a and f_m for the β relaxation in Figure 4b. In Figure 4a we recognize that the f_{mn} for the α_n relaxation of PLA-(5/5) decreases with increasing molecular weight *M*. Therefore, the α_n relaxation can be assigned to the normal mode relaxation due to fluctuation of the end-to-end vector.[1−4]

On the other hand, f_{ms} for the α_s relaxation is almost independent of molecular weight and is seen ca. 10−20 K above T_g. This behavior is typical of the primary relaxation of polymers, and therefore, the α_s relaxation can be assigned to local segmental motions.[3] The β peak locates far below T_g, and the log f_m vs $1/T$ plot is of the Arrhenius type. Therefore, this relaxation is attributed to the secondary relaxation in the glassy state.[3] Since there is no flexible side groups on which dipoles are attached (type-C dipole[1]), the β relaxation is attributed to motions of the main chains.

The log f_{ms} vs $1/T$ plots for the segmental modes have been fitted to the Vogel−Fulcher (VF) equation:[27,28]

$$\log f_{ms} = A - \frac{B}{T - T_o} \qquad (1)$$

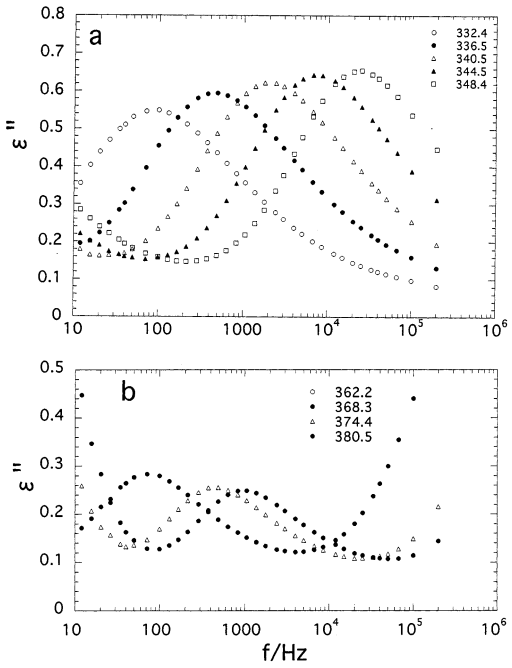

Figure 5. Frequency dependencies of the dielectric loss factor ϵ'' for PLA-8(1/3) in the temperature regions where the segmental modes (a) and the normal mode (b) are observed. Temperatures are indicated in the figures.

Table 2. Vogel−Fulcher Parameters for the Segmental Mode (α_s) of PLA

code	*A*	*B*	T_o
PLA-15(5/5)	12.6	564	277.4
PLA-27(5/5)	12.6	551	280.6
PLA-8(1/3)	11.6	452	285.6
PLA-5(1/3)	11.6	455	281.5

The values of the parameters *A*, *B*, and T_o are determined so that eq 1 fits best and listed in Table 2. The log f_{ms} vs $1/T$ plots for the α_s relaxation of PLA(1/3) and PLA(5/5) are slightly different. The relaxation time also depends slightly on the molecular weight when molecular weight is low due to the effect of chain ends. We will discuss this problem later.

The log f_{mn} vs $1/T$ plots for the normal mode relaxation are also of the Vogel−Fulcher type. Because of the limited number of the data points, we did not determine the Vogel parameters for the normal mode.

Frequency Dependence of ϵ' and ϵ''. Figure 5 shows the representative frequency dependence curves of ϵ'' for PLA-8(1/3). The main ϵ'' curves observed in the temperature range from 330 to 350 K are shown in Figure 5a. Those main loss peaks are due to the α_s relaxation. The loss peaks observed above 350 K are due to the α_n relaxation (Figure 5b). For the samples of PLA-(5/5) the α_n relaxation was not observed clearly in the original ϵ'' curves since the loss due to ionic conduction overwhelmed the loss due to dipolar relaxation. It is known that the ϵ'' due to ionic conduction is proportional to $\sigma_0\omega^{-1}$, where ω is the angular frequency and σ_0 the direct-current conductivity. We have subtracted the contribution of the ionic conduction assuming that σ_0 is independent of frequency. Parts a and b of Figure 6 show the ϵ'' curves of PLA-27(5/5) for the α_s and α_n relaxations, respectively, and the ϵ'' curve for the normal mode (Figure 6b) has been thus obtained.

The ϵ'' curves for the α_s relaxation have a typical shape for amorphous polymers: the distribution of

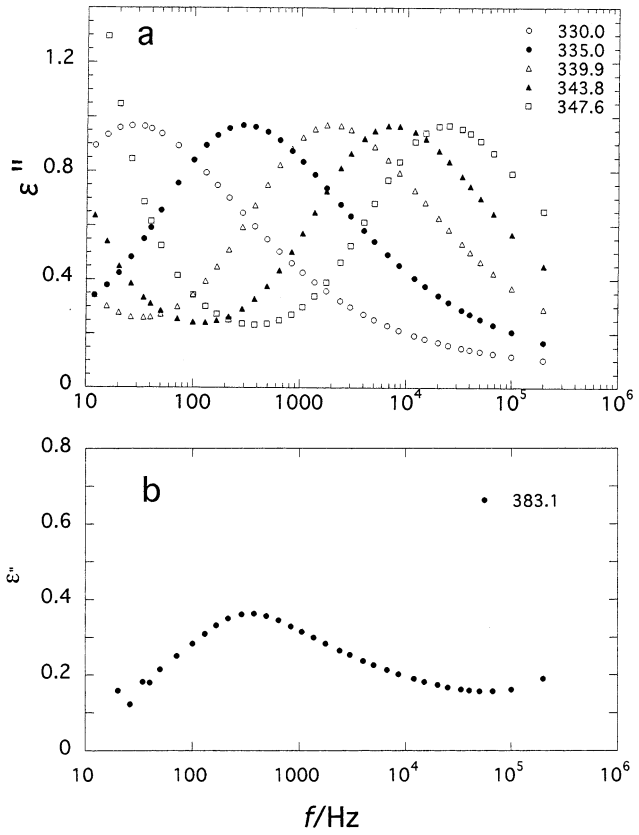

Figure 6. Frequency dependencies of the dielectric loss factor ϵ'' for PLA-27(5/5): (a) the ϵ'' curves in the temperature region where the a_s relaxation is observed; (b) the ϵ'' curves in the temperature region where the α_n relaxation is observed. Temperatures are indicated in the figures.

Table 3. Parameters of Havriliak−Negami Equation (Eq 2) and Kohlrausche−Williams−Watts Equation (Eq 3) for the Segmental Mode (α_s) at Temperatures Indicated

code	*T*	α	β	β_{KWW}
PLA-15(5/5)	338.5	0.760	0.522	0.428
PLA-27(5/5)	337.9	0.764	0.466	0.395
PLA-47(5/5)	339.2	0.718	0.483	0.401
PLA-5(1/3)	337.4	0.660	0.579	0.399
PLA-8(1/3)	338.5	0.718	0.483	0.381

relaxation times in the high-frequency side is broader than that of low-frequency side. We have attempted to fit the ϵ'' curves for the α_s relaxation to the Havriliak−Negami (HN) equation:[29]

$$\epsilon^* - \epsilon_\infty = \frac{\Delta\epsilon_s}{[1 + (i\omega\tau)^\alpha]^\beta} \tag{2}$$

Here ϵ^* ($=\epsilon'-i\epsilon''$) is the complex dielectric constant, ϵ_∞ the high-frequency dielectric constant, and $\Delta\epsilon_s$ the relaxation strength for the segmental mode, and α, β, and τ are the parameters. These parameters are listed in Table 3. The parameters α and β decreased slightly with decreasing temperature.

It is known that the inverse Fourier transform of the HN equation (eq 2) can be represented by the Kohlrausche−Williams−Watts (KWW) equation $\phi(t)$:[30,31]

$$\phi(t) = \exp\left(-\frac{t}{\tau_{KWW}}\right)^{\beta_{KWW}} \tag{3}$$

where β_{KWW} is the parameter describing the nonexponential character of the correlation function and τ_{KWW}

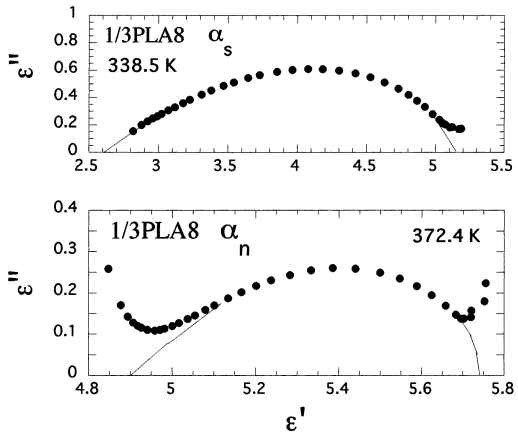

Figure 7. Cole−Cole plot for the segmental mode (upper) and that for the normal mode (bottom) of PLA-8(1/3) at temperatures indicated The values of the relaxed dielectric constant ϵ_R and unrelaxed dielectric constant ϵ_U are determined by extrapolation of the plots as shown in the figure.

Table 4. Relaxation Strength for the Normal Mode $\Delta\epsilon_n$ and Segmental Mode $\Delta\epsilon_s$ of PLA8(1/3) at Temperatures Indicated

T	$\Delta\epsilon_n$	$\Delta\epsilon_s$	ϵ_R	ϵ_U
372.4	0.84		5.74	4.90
338.5		2.54	5.14	2.61

is the nominal relaxation time. The HN and KWW parameters are listed in Table 3. As seen in this table, β_{KWW} is found to be 0.41 ± 0.01 for all samples. In the amorphous state, the KWW equation was explained by considering cooperative motions of segments.[32] Several models[33,34] of cooperative reorientation of segments were also developed for explanation of the VF equation and the KWW correlation function, but origins for these behaviors have not been perfectly understood.

Parallel and Transverse Dipole Moments. The relaxation strengths for the α_s and α_n relaxations were determined from the Cole−Cole plots and listed in Table 4. The representative Cole−Cole plots for PLA-8(1/3) and PLA-5(1/3) are shown in Figure 7. The relaxation strength $\Delta\epsilon_n$ for the normal mode in the electrostatic unit (esu) is given by

$$\frac{\Delta\epsilon_n}{C} = \frac{4\pi N_A \mu^2 \langle r^2 \rangle}{3k_B TM} F \tag{4}$$

where C is the concentration in the unit of g/mL, μ the dipole moment per unit contour length, $\langle r^2 \rangle$, the mean square end-to-end distance, and F the internal field factor. For undiluted polymers C is equal to the density ρ. Stockmayer and Baur proposed that F for solutions of type-A polymers is given by

$$F = \frac{(\epsilon + 2)^2}{9} \tag{5}$$

where ϵ is the dielectric constant of solvent. For undiluted polymers, it is not clear whether this equation is applicable. This equation originates from the internal field factor proposed by Onsager[35] and corresponds to the case where the relaxed dielectric constant ϵ_R is approximately equal to unrelaxed dielectric constant ϵ_U. For undiluted PLA, ϵ may be replaced with the unrelaxed dielectric constant for the normal mode relaxation.

The theories of the internal field[35,36] were developed on the basis of assumption that a test dipole is put at the center of a spherical vacuum cavity formed in a dielectrics. The size of the cavity is similar to the test dipole. The dipole is subjected to an extra field due to the charges formed on the surface of the cavity, and hence, the value of F becomes larger than unity. However, we encounter a difficulty in applying those models to the polarization of type-A chains, since it is physically difficult to imagine that a test type-A chain is put in a vacuum cavity of the size of the radius of gyration of the chain. We should use a model that the cavity is filled with solvent in the case of solutions or with interpenetrated chains in the case of bulk systems. Therefore, F for the normal mode relaxation should be smaller than the values of F proposed for simple molecules. In fact, it was observed experimentally that F for solutions of poly(2,6-dichlorophenylene oxide) was close to unity.[37] Similar result was reported for solutions of rodlike poly(hexyl isocyanate) by Takada et al.[38]

Paying attention to the theoretical background mentioned above, we analyzed the relaxation strength of PLA. First it is needed to determine the parallel (p_A) and transverse (p_B) components of the monomeric dipole with respect to the virtual bond (C_1- - -C_4). Baysal and Stockmayer[39] calculated p_A and p_B from the relaxation strength for solution of poly(ϵ-caprolactone) assuming eq 5 and reported that $p_A = 0.64$ D and $p_B = 1.60$ D (Debye unit = 10^{-18} cgs esu). They also reported that p_A becomes 0.90 D with $F = 1$. We estimated p_A and p_B by means of the semiempirical molecular orbital methods AM1 and PM3[40,41] for butylester of valeric acid CH_3-$(CH_2)_3$−CO−O−$(CH_2)_3$−CH_3. The parallel and transverse components with the AM1 method become $p_A = 0.45$ and $p_B = 1.69$ D (Debye unit), respectively. On the other hand the PM3 method gives $p_A = 0.41$ and $p_B = 1.75$ D. The total dipole moment of the ester group calculated with AM1 is 1.75 D and that with PM3 is 1.80 D. The experimental dipole moment of the ester group is reported to be 1.80 D.[42] Thus, PM3 is the better model for esters. Since μ is equal to p_A divided by the length of the virtual bond b_v (=0.369 nm), μ becomes 1.11×10^{-11} esu for the PM3 method and 1.22×10^{-11} esu for the AM1 method. The values of p_A obtained here are smaller than that reported by Baysal and Stockmayer.[39]

To determine F from the relaxation strength $\Delta\epsilon_n$ for the normal mode listed in Table 4, we need the data of $\langle r^2 \rangle / M$ appearing in eq 4. Since the excluded volume effect is shielded in the undiluted state, $\langle r^2 \rangle / M$ is independent of the molecular weight.[43] The characteristic ratio C_∞ of PLA is defined by

$$\langle r^2 \rangle = C_\infty N b_v^2 \tag{6}$$

where N is the degree of polymerization and b_v the length of the virtual bond (=0.369 nm). The unperturbed dimension of PLA was calculated by Brant et al. based on the assumption of the rotational isomeric state model (RIS).[44,45] They reported $C_\infty = 2.05$, indicating that the PLA chains are very flexible. Joziasse et al. measured the light scattering on solutions of racemic PLA and poly(*l*-lactic acid) in acetonitrile.[46] They reported that C_∞ depends on the *l*/*d* lactide ratio and increases from 4.34 (9.5) for *d*,*l*-PLA to 5.39 (11.8) for *l*-PLA. Here the values indicated in the brackets are those defined as ref 45. They stressed that those higher values of C_∞ than

Table 5. Internal Field Factor *F* from Data of $\langle r^2\rangle/M$ of PLA

data source	tacticity	C_∞	F
Brant et al. (ref 44)	*l*	2.05	3.58
Joziasse et al. (ref 45)	*d*,*l*	4.34	1.69
(ref 45)	*l*	5.39	1.36
Yang et al. (ref 46)	*l*	3−5.5	2.4−1.3
Ren et al. (ref 48)	*d*,*l*	4.07	1.8

that reported by Brant et al. are consistent with the brittle nature of PLA. Later Yang et al. estimated C_∞ of PLA to be 3 (7) to 5.5 (12) from the confomational energy measured by the Raman spectroscopy.[47] Recently, we measured the intrinsic viscosity $[\eta]$ of PLA-(1/3) in a good solvent benzene.[48] The result can be cast into the Mark−Houwink−Sakurada equation $[\eta] = KM^\alpha$ with $K = 1.10 \times 10^{-2}$mL/g and $\alpha = 0.806$. Using this result, $\langle r^2\rangle/M$ is estimated assuming the Flory−Fox equation[49]

$$\langle s^2\rangle^{3/2} = \frac{M[\eta]}{6^{3/2}\Phi} \tag{7}$$

where $\langle s^2\rangle$ is the mean square radius of gyration and Φ the constant. Assuming that $\Phi = 2.5 \times 10^{23}$ cgs and that $\langle r^2\rangle \approx 6\langle s^2\rangle$, we have calculated $\langle r^2\rangle/M$ to be 7.7×10^{-17} at $M = 8000$. Since the molecular weight is relatively low, this value is close to that in the unperturbed state and C_∞ is estimated to be 4.1.

We have calculated F with $\mu = 1.11 \times 10^{-11}$ esu obtained by the PM3 method and the data of C_∞ mentioned above. The results are listed in Table 5. Here we used $\rho = 1.246$ g cm^{-3}. As is seen in this table, F ranges from 1.3 to 3.6.

We compare those values of F with the theoretical F. The value of ϵ in eq 5 is considered to be the unrelaxed dielectric constant ϵ_U (=4.90) for the normal mode. Then F becomes 5.3. As mentioned above we proposed that $F = 1$. Comparing those theoretical values with the results listed in Table 5, we see that the experimental F is close to unity but is not exactly one. Thus, the theory of F for the normal mode relaxation is needed. We also note that if we use $\mu = 1.22 \times 10^{-11}$ esu obtained by the AM1 method, F ranges from 1.1 to 3.0. Thus, it is also required to check the reliability of the PM3 method.

Relaxation Strength for the Segmental Mode. The relaxation strength $\Delta\epsilon_s$ for the α_s relaxation was determined by using the Cole−Cole plot to be 2.53 for PLA-8 at 339 K. For the relaxation strength $\Delta\epsilon_s$ associated with local motions, the Onsager−Kirkwood equation has been used:[35,50]

$$\Delta\epsilon_s = \frac{4\pi N g p_B^2}{3k_B T}\frac{(\epsilon_U + 2)^2\epsilon_R}{3(2\epsilon_R + \epsilon_U)} \tag{8}$$

where N is the number of the monomeric unit in unit volume, g, the Kirkwood correlation parameter, p_B the type-B dipole moment, ϵ_U the unrelaxed dielectric constant, and ϵ_R the relaxed dielectric constant. From the data of $\Delta\epsilon_s$, the value of gp_B^2 is determined to be 0.96 D^2. As mentioned above we calculated p_B with the PM3 and AM1 methods to be 1.76 and 1.69 D, respectively. By using these values g is determined to be 0.31 and 0.34 for the dipoles calculated with the PM3 and AM1 methods, respectively. If the g factor is mainly due to the intramolecular interactions, we can conclude that the transverse dipoles tend to orient antiparallel. Looking at the structure of PLA shown in Figure 1, we see that the PLA molecules tend to take the planar zigzag conformation. It is needed to assess the contribution of intermolecular interactions to the g factor.

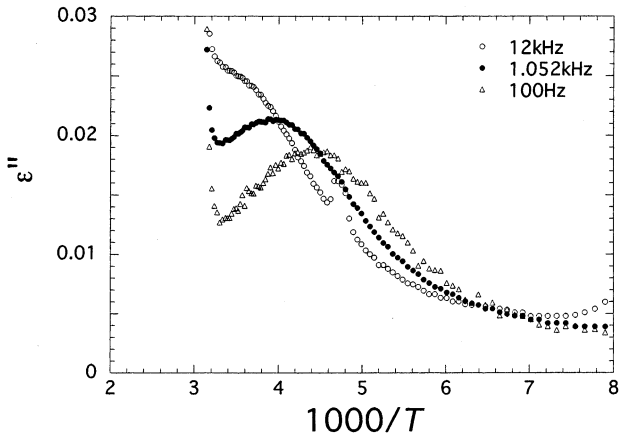

Figure 8. Plots of the dielectric loss factor ϵ'' against $1/T$ in the β relaxation region for PLA-8(1/3). The relaxation strength is determined from the area in the right-hand side of the peak

Effective Dipole Moment for the β Relaxation. The frequency dependence curve of ϵ'' for the β relaxation is rather weak and broad. To determine the relaxation strength $\Delta\epsilon$ for this relaxation process, we plotted ϵ'' against the inverse of temperature and $\Delta\epsilon$ was determined from the area of the peak to be 0.20 ± 0.01:

$$\Delta\epsilon = \frac{2E_a}{\pi R}\int_0^\infty \epsilon''\, \mathrm{d}(1/T) \tag{9}$$

where E_a is the activation energy and R the gas constant. Figure 8 shows the representative plots for PLA-8. As pointed out for Figure 4b, the temperature dependence of the average relaxation frequency f_m for the β relaxation is given by the Andrade equation. The activation energy was determined to be 41.1 kJ/mol. Because PLA chains do not possess type-C dipoles, the β relaxation is assigned to twisting motions of the main chains which is termed as "local mode relaxation" by Yamafuji and Ishida.[51] They proposed a model for the secondary relaxation in glassy states assuming highly damped torsional oscillations of the chain backbone.

We assume that the average angle for twisting motions of the main chain is $\pm\phi$. Then the effective dipole moment p_{eff} is defined by

$$p_{eff} = p_B \sin\phi \tag{10}$$

where p_B is the transverse component of the dipole moment of the ester group and is already calculated above to be 1.76 ± 0.3 D. We have calculated the effective dipole moment p_{eff} by using eq 8 to be 0.30 D. Here we replaced gp^2 of eq 8 by p_{eff}^2. Then with eq 10, we obtain ϕ to be 11°. This small amplitude is consistent with the relatively low activation energy for the β relaxation.

Behavior of Normal Mode Relaxation. As mentioned above, the normal mode relaxation (α_n) and the segmental mode relaxations (α_s) were observed at about 390 and 340 K, respectively. From the frequency dependence curves of the dielectric constant ϵ' and the loss factor ϵ'' in those temperature range, we constructed the

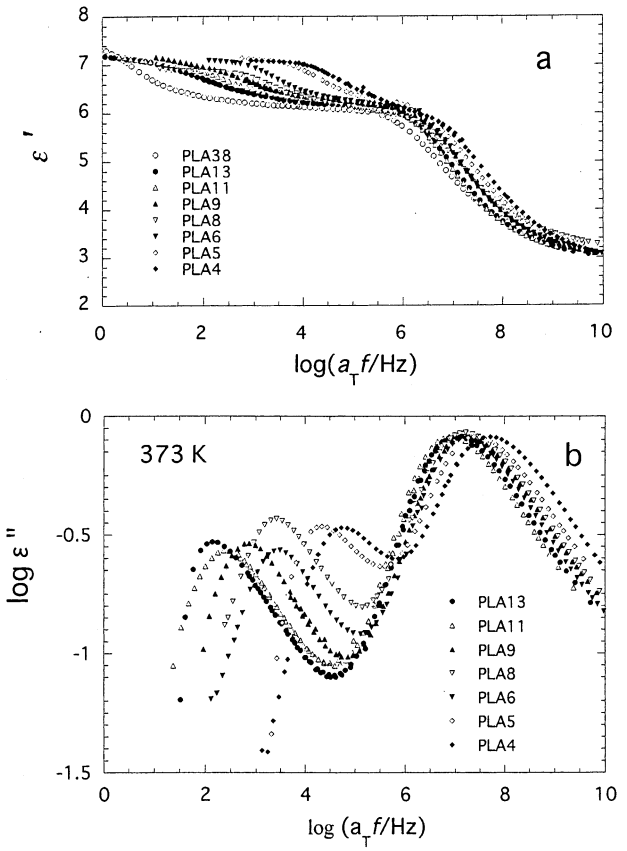

Figure 9. Representative master curves of ϵ' and ϵ'' of the PLA samples at 373.2 K: (a) ϵ' curves; (b) ϵ'' curves.

master curves at 373.2 K after correction of the electric conductivity. As mentioned above, we found that the dielectric loss (ϵ'') curves for the segmental mode broadened slightly with decreasing temperature. Therefore, the time−temperature superposition principle does not hold perfectly in the region of the segmental mode relaxation. Nevertheless, the master curves presented here are useful for looking at the behavior ranging over the regimes of the segmental and the normal modes. For quantitative analyses we used the original ϵ' and ϵ'' curves measured at various temperatures. The master curves of ϵ' and ϵ'' thus constructed are shown in Figure 9. The loss peaks at the low- and high-frequency sides correspond to the normal and segmental modes, respectively.

We see that f_{mn} shifts to the low-frequency side with increasing molecular weight M_w but f_{ms} for the segmental mode is almost independent of M_w. We see that f_{ms} increases slightly when the molecular weight is low. This is due to the effect of chain ends creating more free volume than the high molecular weight samples. We also see that f_{ms} depends slightly on the conditions of the polymerization of PLAs and hence f_{ms} for the samples fractionated from S1 to S4 samples are slightly different. This difference may be ascribed to the slight difference in the microstructure of the chains. In fact, the specific rotatory power of S1 to S4 samples were found to be slightly different as shown in Figure 10. We may assume that the mechanisms of the dynamics of those samples obtained by fractionation from S1 to S4 samples are the same, but the friction for the mobility of them changes slightly from sample to sample.

Relaxation Time for the Normal Mode in the Isofriction State. To examine the molecular weight

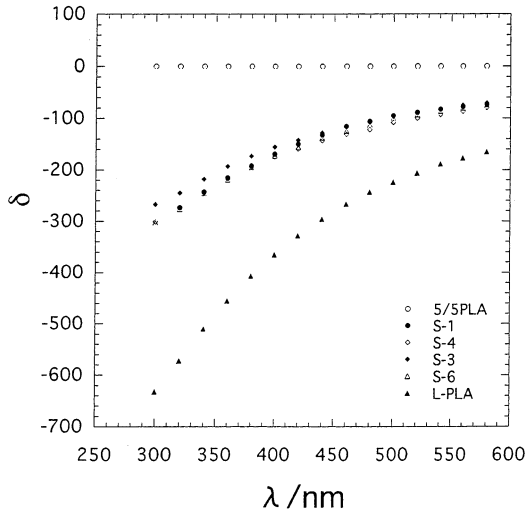

Figure 10. Wavelength λ dependence of the specific rotatory power δ of the PLA samples.

dependence of the normal mode relaxation times, it is required to correct them to those in the isofriction state. Generally the relaxation time τ for the large scale motions can be represented by a form[52]

$$\tau = \zeta(T)F(N_e) \tag{11}$$

where $\zeta(T)$ is the friction factor depending only on temperature T and F is the structural factor depending on the architecture of the chains and on the number of entanglements N_e ($=M/M_e$). Here M_e denotes the molecular weight between entanglement. In the previous studies on polyisoprene,[53] it was found that f_{mn} for the normal mode and f_{ms} for the segmental mode changed parallel with temperature when temperature was higher than $T_g + 30$ K. For the present PLA samples, T_g ranges from 300 to 320 K and therefore the relaxation time τ_s for the segmental mode in the range above 350 K is expected to be proportional to the monomeric friction coefficient ζ. Assuming this relationship, we attempted to correct the normal mode relaxation times τ_n of the PLA samples into those ($\tau_{n\zeta}$) in the isofriction state. The ζ in the high molecular weight samples of the S1 group were taken as the standard state. It is noted that the precise determination of f_{ms} for the segmental mode was made using the frequency dependence curves of ϵ'' measured at various temperatures and the master curve was not used. If necessary, f_{ms} was extrapolated by using the Vogel−Fulcher equation (eq 1).[27,28] Thus, the shift factor for the correction of friction can be given by

$$\frac{\zeta}{\zeta^o} = \frac{f_{ms}^o}{f_{ms}} \tag{12}$$

where the superscript o denotes the standard state. The normal mode relaxation time was reduced to $\tau_{n\zeta}$ by multiplying this shift factor to the observed τ_n.

The $\tau_{n\zeta}$'s thus determined at 373.2 K are plotted against the weight-average molecular weights M_w in Figure 11. Unfortunately the plots in low molecular weight region are scattered and the break of the plots corresponding to the characteristic molecular weight M_c is not very clear. We have drawn the smoothed curve as shown in Figure 11, and M_c is determined to be 13 000. However we have a good reason that M_c is ca.

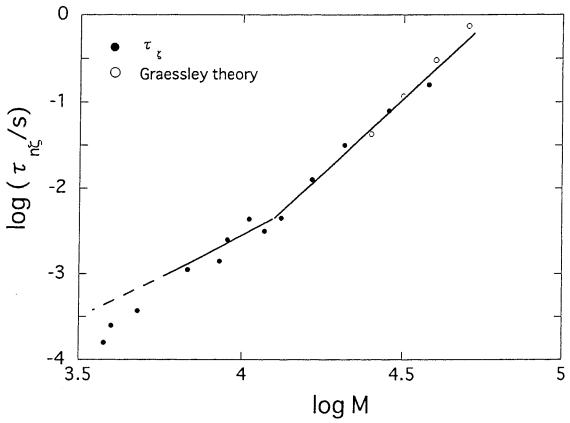

Figure 11. Molecular weight dependence of the dielectric normal mode relaxation times $\tau_{n\zeta}$ corrected to the isofriction state.

15 000 as will be described in the section of the viscoelastic properties. In the range of $M > M_c$, the normal mode relaxation time $\tau_{n\zeta}$ is approximately proportional to $M_w^{3.5}$. A similar dependence of $\tau_{n\zeta}$ on M_w was observed for the dielectric normal mode relaxation of *cis*-polyisoprene in the M range above its characteristic molecular weight M_c.[2−5] The exponent was 3.7 and slightly higher than PLA. Below M_c we have drawn the line of slope 2.0 according to the Rouse model:[54]

$$\tau_R = \frac{\zeta b^2 N^2}{3\pi^2 k_B T} \tag{13}$$

Here ζ, b, N, and k_BT are the friction coefficient per bead, the distance between beads, the number of beads, and thermal energy, respectively. It is seen in Figure 11 that, in the low molecular weight samples with M_w less than 5000, the relaxation time is lower than the values predicted by eq 12. Since the correction to the isofriction state has already been made, the lowering of the relaxation time below the theoretical value cannot be ascribed to the effect of friction. The origin of this discrepancy is not clear at present.

For entangled chains the M dependence of the longest relaxation time is explained by the reptation model proposed by de Gennes and Doi−Edwards.[55,56] The tube disengagement time τ_d is given by

$$\tau_d = \frac{3\tau_R^e M^3}{M_e^3} \tag{14}$$

where τ_R^e is the Rouse relaxation time at $M = M_e$. As is well-known, the theoretical exponent 3.0 is lower by 0.5 than the observed exponent for the viscoelastic and the dielectric normal mode relaxations.

By using the dilute blends of polyisoprene in polybutadiene or binary blends of polyisoprene,[57,58] it was demonstrated experimentally that the higher exponents can be explained by the constraint release model proposed by Graessley.[59] The relaxation time for the constraint release is represented as

$$\tau_{CR} = \left(\frac{2\Lambda}{\pi^2}\right)\left(\frac{N}{N_e}\right)^2 \tau_d \tag{15}$$

where Λ is a constant related to the rate of the constraint release and is a function of the gate number

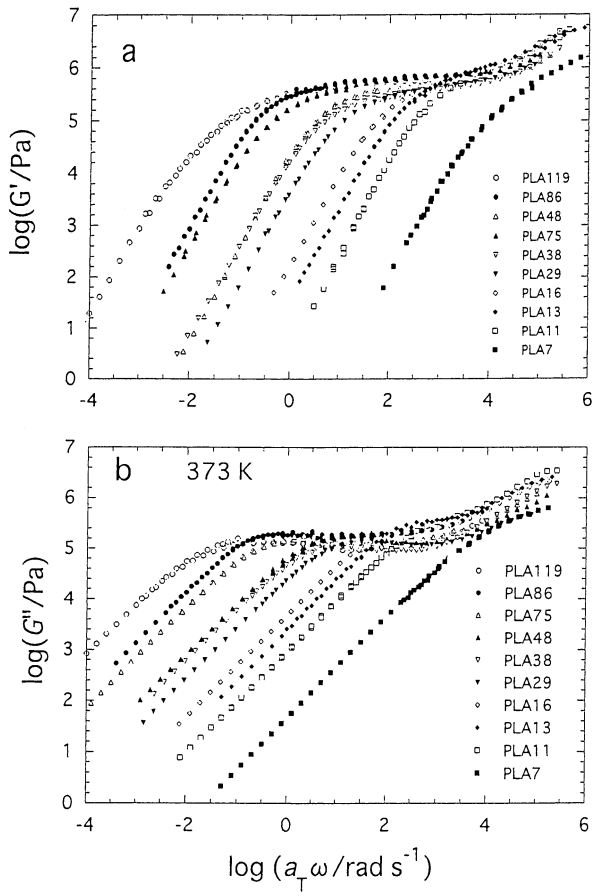

Figure 12. Master curves of G' and G'' of the PLA samples at 373.2 K. (a) G' curves. (b) G'' curves.

z for local jumps of the beads, and N_e is the number of beads between entanglements. The relaxation time is determined through the competition of the two relaxation processes, i.e., the reptation and the constraint release:

$$1/\tau = 1/\tau_d + 1/\tau_{cr} \tag{16}$$

$$\tau = \tau_d\left[\frac{2\Lambda M^2}{2\Lambda M^2 + \pi^2 M_e^2}\right] \tag{17}$$

If the constant Λ is assumed to be 0.185 corresponding to the gate number $z = 3$, the slope of $\tau_{n\zeta}$ vs M_w becomes 3.5 as shown in Figure 11. The calculation was made with $M_e = 7700$ by assuming that the front factor is adjustable. Although the Graessley theory explains the slope, it does not quantitatively agree with the experiment around M_c. For polyisoprene the M_w dependence of $\tau_{n\zeta}$ was explained with $z = 4$.[57,58] Thus, the results on polyisoprene and on PLA are explained in terms of the same model. As discussed in the introductory section PLA is a type-A1 polymer and polyisoprene a type-A2 polymer. As far as the M_w dependence of $\tau_{n\zeta}$ is concerned, no significant difference is seen between the type-A1 and A2 polymers.

Viscoelastic Relaxation. Figure 12 shows the double logarithmic plots of the storage shear modulus G' and loss modulus G'' at 373.2 K against angular frequency ω for the PLA samples. In Figure 12, we see that the rubbery plateau region increases with increasing molecular weight as is commonly observed for amorphous

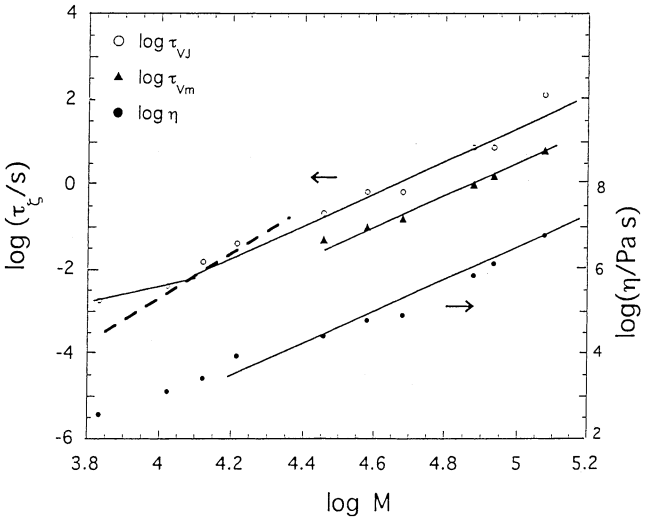

Figure 13. Molecular weight dependencies of the viscoelastic relaxation time and the zero shear viscosity. $\tau_{vJ} = J_e°\eta^2$, where $J_e°$ is the steady compliance and η the zero shear viscosity. τ_{vm} is defined by $\tau_{vm} = \omega_m^{-1}$, where ω_m is the loss maximum angular frequency. The dashed line indicates the viscoelastic relaxation time calculated with eq 19 by using the data of η.

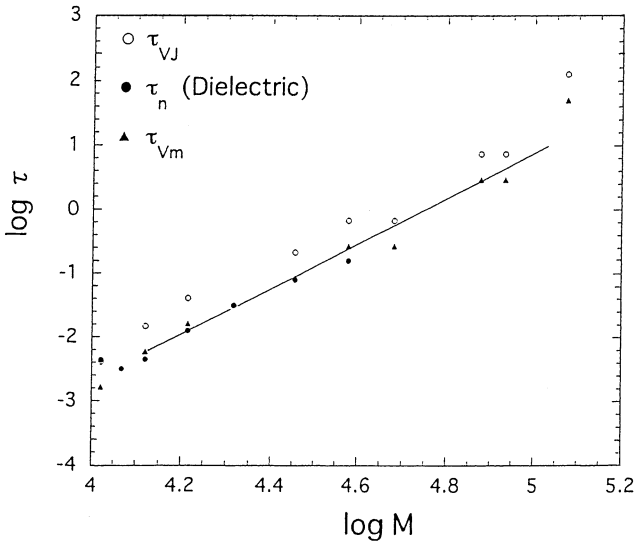

Figure 14. Comparison of the dielectric and viscoelastic relaxation times in the terminal region.

polymers. The rubbery plateau modulus $G_N°$ is related to the molecular weight between entanglements M_e by

$$G_N^o = \frac{\rho RT}{M_e} \tag{18}$$

where ρ is the density and R the gas constant. From the average value of $G_N^o = 5.1 \times 10^5$ Pa, M_e becomes 7.7×10^3. The zero shear viscosity η was determined from the value of G'' in the region where G'' is proportional to angular frequency ω. The molecular weight dependence of η is shown in Figure 13. The slope is ca. 3.5 and therefore the most of the PLA samples used in this study are in the entangled state. The slope is slightly higher than the exponent expected from the 3.4 power law. Justin et al.[22] reported the viscoelastic measurements on *l*-PLA and found that the M_c is 16 000 and that zero shear viscosity is proportional to $M^{4.0}$ in the range of $M > M_c$.

The terminal relaxation time τ_v was determined in two ways. First we used the relationship of $\tau_{vJ} = J_e°\eta^2$ where $J_e°$ is the steady compliance and η the zero shear viscosity. Second the terminal relaxation time is determined with $\tau_{vm} = \omega_m^{-1}$ where ω_m is the angular frequency of maximum G''. The molecular weight dependencies of τ_{vJ} and τ_{vm} are shown in Figure 13. The slope of the plot is 3.5 in consistent with the exponent for the viscosity. As is well know the double logarithmic plot of η or τ_{vJ} against M_w exhibits a break at a characteristic molecular weight M_c. In Figure 13 we do not see clear break point around M_c. From the value of M_e determined above and the empirical rule of $M_c \approx 2M_e$, M_c becomes 15 000.

According to the Rouse theory,[54] the viscoelastic relaxation time τ_v in $M < M_c$ is given by

$$\tau_v = \frac{6\eta M}{\pi^2 \rho RT} \tag{19}$$

where ρ and R are the density and gas constant. This equation is used to estimate M_c. The values of η given by the smoothed line are substituted for η of eq 19 to calculate τ_v. We expect that τ_v thus calculated should be higher than the observed viscoelastic relaxation time since the viscosity data in the entangled regime have been used. But the calculated and observed τ_v become the same at M_c. The calculated τ_v is plotted in Figure 13 by the dashed line. As is seen in Figure 13 the dashed line and observed τ_{vJ} coincide at $M = 16\,000$, indicating $M_c = 16\,000$ which approximately agrees with M_c (=13 000) determined from the dielectric data.

Comparison of the Dielectric and Viscoelastic Relaxations. The dielectric normal mode relaxation time τ_n and the viscoelastic relaxation times τ_{vJ} and τ_{vm} are compared in Figure 14. We see that τ_{vJ} is longer than τ_n but τ_{vm} coincides with τ_n. Since τ_{vJ} is the average relaxation time defined by $\Sigma g_i\tau_i^2/\Sigma g_i\tau_i$, τ_{vJ} should be shorter than τ_n, which is close to the longest relaxation time.[60] Here g_i denotes the intensity of the viscoelastic relaxation spectrum. The present result is reverse of our expectation. The reason for this result is not clear, and we consider that the distribution of molecular weight might be the origin of the discrepancy. Ngai found that the viscoelastic fuctions in the terminal region are not superposable.[32] The present result may be partly due to this effect.

Finally we compare the dielectric and viscoelastic relaxation spectra using Figures 9b and 12b. It is seen that the G'' curves are much broader than the ϵ'' curves. This is partly due to the overlapping of the contribution of the wedge type spectrum in the viscoelastic relaxation. However, the G'' curves of high molecular weight PLAs having G'' peaks far from the wedge type spectra are still broader than the ϵ'' curve for the dielectric normal mode. Thus, we conclude that the viscoelastic relaxation spectra are broader than the dielectric relaxation spectra. This behavior is similar to that of polyisoprene.[7−10]

Conclusion

We have investigated the dielectric and viscoelastic relaxation behavior of poly(*d*,*l*-lactic acid) (PLA) having a unique structure that the whole repeat unit can be regarded as a virtual bond. Because of this structure, PLA can be classified as a type A1 polymer in which the overall dipole moment of the chain is exactly proportional to the end-to-end vector of the chain. The

data indicate that PLA exhibits three dielectric relaxations, i.e., the normal mode relaxation (α_n) at about 380 K, the segmental mode relaxation (α_s) around 345 K, and the secondary relaxation (β) around 240 K at 1 kHz. The temperature dependencies of the relaxation frequencies f_m for both the normal and segmental modes conform to the Vogel−Fulcher (VF) equation. On the other hand the relaxation time for the β process conforms to the Andrade equation. The parameters for the relaxation functions such as the Havriliak−Negami and Kohlrausche−Williams−Watts equations have been determined for the α_s relaxation. The values of these parameters are found to be similar to those of other amorphous polymers, indicating that the effect of the unique structure of PLA does not affect strongly on the behavior of local motions. We have analyzed the dielectric relaxation strengths for the mormal mode and segmental mode using the parallel and perpendicular components of the monomeric dipole calculated with the aid of the PM3 and AM1 methods. From the dielectric relaxation strength and the reported data of the characteristic ratios of PLA, the internal field factor F is found to be smaller than the F proposed by Stockmayer. The value of F ranges from 1.3 to 3 and is close to unity. However the uncertainty on the reliability of the semiempirical molecular orbital methods still remains and the theoretical studies on F are needed. From the relaxation strength for the α_s relaxation the Kirkwood correlation factor g is determined to be 0.3. The β relaxation is due to the local twisting motions of the PLA chains in the glassy state. The amplitude of the twisting motion becomes 11°.

The main interest of this study has been in the behavior of the normal mode relaxation of PLA belonging to type-A1 polymers. From the molecular weight dependence of the dielectric normal mode relaxation time τ_n the characteristic molecular weight M_c is determined to be 13 000. Both the dielectric normal mode relaxation time τ_n and the viscoelastic relaxation time τ_v increase with molecular weight M in proportion to $M^{3.5} \pm 0.2$ in the range of $M > M_c$. The dielectric relaxation time τ_n coincides with the viscoelastic relaxation time τ_{vm} determined from the loss maximum frequency. The distribution of the relaxation times for the viscoelastic relaxation is broader than that for the dielectric normal mode relaxation. From those results, we conclude that the dielectric behavior of PLA is very similar to that of polyisoprene which is a type-A2 polymer. We conclude that there is no essential difference between the normal mode relaxations of PLA and polyisoprene. Since polyisoprene possesses a structure very similar to type-A1 polymers, we should postpone the conclusion that there is no difference between the type A1 and A2 polymers until the dielectric data for a typical type-A2 polymer such as poly(ϵ-caprolactone) are obtained.

Acknowledgment. J.R. thanks the Ministry of Education, Culture, Sports, Science, and Technology of Japan for a scholarship.

References and Notes

(1) Stockmayer, W. H. *Pure Appl. Chem.* **1967**, *15*, 539.
(2) North, A. M. *Chem. Soc. Rev.* **1972**, *1*, 49.
(3) McCrum, N. G.; Read, B. E.; Williams, G. *Anelastic and Dielectric Effects in Polymeric Solids*; Dover Publication: New York, 1967; Chapter 5.
(4) Adachi, K.; Kotaka, T. *Prog. Polym. Sci.* **1993**, *16*, 585.
(5) Jones, A. A.; Stockmayer, W. H.; Molinari, R. J. *J. Polym. Sci. Symp.* **1976**, *54*, 227.
(6) Urakawa, O.; Adachi, K.; Kotaka, T.; Takemoto, Y.; Yasuda, H. *Macromolecules* **1994**, *27*, 7410.
(7) Adachi, K.; Kotaka, T. *Macromolecules* **1984**, *17*, 120.
(8) Adachi, K.; Kotoka, T. *Macromelecules* **1985**, *18*, 466.
(9) Imanishi, Y.; Adachi, K.; Kotoka, T. *J. Chem. Phys.* **1988**, *89*, 7593.
(10) Bose, D.; Kremer, F. *Macromelecules* **1990**, *23*, 829.
(11) Flory, P. J.; Williams, A. D. *J. Polym. Sci. A2* **1967**, *5*, 399.
(12) Baur, M. E.; Stockmayer, W. H. *J. Chem. Phys.* **1965**, *43*, 4319.
(13) Burke, J. J.; Stockmayer, W. H. *Macromolecules* **1969**, *3*, 647.
(14) Schlosser, E.; Schonhals, A. *Prog. Colloid Polym. Sci.* **1993**, *91*, 158.
(15) Hayakawa, T.; Adachi, K. *Polymer* **2001**, *42*, 1725.
(16) Adachi, K.; Kotaka, T. *Macromolecules* **1983**, *16*, 1936.
(17) North, A.; Phillips, P. J. *Trans. Faraday Soc.* **1968**, *18*, 371.
(18) Uzaki, S.; Adachi, K.; Kotaka, T. *Macromolecules* **1988**, *21*, 153.
(19) Adachi, K.; Yoshida, H.; Fukui, F.; Kotaka, T. *Macromolecules* **1990**, *23*, 3138.
(20) Yager, W. A.; Baker, W. O. *J. Am. Chem. Soc.* **1942**, *64*, 2164.
(21) Wurstlin, F. *Kolloid Z.* **1948**, *110*, 71.
(22) Justin, J. C.; Michael, E. M. *J. Polym. Sci.: Part B* **1999**, *37*, 1803.
(23) Okada, M. *Prog. Polym. Sci.* **2002**, *27*, 87.
(24) Hausberger, A. D.; Deluca, P. P. *J. Pharmaceut. Biomed.* **1995**, *13*, 747.
(25) Leenslag, J. W.; Pennings, A. J.; Bos, R. R. M.; Rozema, F. R.; Boering, G. *Biomaterials* **1987**, *8*, 70.
(26) Ajioka, M.; Enomoto, K.; Suzuki, K.; Yamaguchi, A. *Bull. Chem. Soc. Jpn.* **1995**, *68*, 2125.
(27) Vogel, H. *Phys. Z.* **1921**, *22*, 645.
(28) Fulcher, J. G. *J. Am. Ceram. Soc.* **1925**, *8*, 339.
(29) Havriliak, S.; Negami, S. *J. Polym. Sci.: C* **1966**, *14*, 99.
(30) Kohlrausche, F. *Prakt. Phys.* **1955**, *1*, 129.
(31) Williams, G.; Watts, D. C. *Trans. Faraday Soc.* **1970**, *66*, 80.
(32) Ngai, K. *J. Non-Cryst. Solids*, **2000**, *275*, 7.
(33) Adachi, K. *Macromolecules* **1990**, *23*, 1816.
(34) Matsuoka, S.; Quan, X. *Macromelecules* **1991**, *24*, 2770.
(35) Onsager, L. *J. Am. Chem. Soc.* **1936**, *58*, 1486.
(36) Bottcher, C. J. F.; Bordewijk, P. *Theory of Electric Polarization*; Elsevier: New York, 1978, Vol. 1.
(37) Adachi, K.; Okazaki, H.; Kotaka, T. *Macromolecules* **1985**, *18*, 1687.
(38) Takada, S.; Itou, T.; Chikiri, H.; Einaga, Y.; Teramoto, A. *Macromelecules* **1989**, *22*, 973.
(39) Baysal, B. M.; Stockmayer, W. H. *Macromolecules* **1994**, *27*, 7429.
(40) Dewar, M. J. S.; Zoebisch, E. G.; Healy, E. F.; Stewart, J. J. P. *J. Am. Chem. Soc.* **1985**, *107*, 3902.
(41) Stewart, J. J. P. *J. Comput. Chem.* **1991**, *12*, 320.
(42) Smyth, C. P. *Dielectric Behaviour and Structure*; McGraw-Hill: New York: 1955; Section 9.10, pp 303−311.
(43) Hayashi, H.; Flory, P. J.; Wignell, G. D. *Macromelecules* **1983**, *16*, 1328.
(44) Brant, D. A.; Tonelli, A. E.; Flory, P. J. *Macromelecules* **1969**, *2*, 228.
(45) Brant et al. reported the value of C_∞ defined by $C_\infty = \langle r^2 \rangle / N(b_{CC}^2 + b_{CO}^2 + b_{OC}^2)$. The repoorted value was converted into C_∞ defined by eq 6.
(46) Joziasse, C. A.; Veenstra, H.; Grijpma, D. W.; Penning, A. J. *Macromol. Chem. Phys.* **1996**, *197*, 2219.
(47) Yang, X.; Kang, S.; Hsu, S. L.; Stidham, H. D.; Smith, P. B.; Leugers, A. *Macromolecules* **2001**, *34*, 5037.
(48) Ren, J.; Urakawa, O.; Adachi, K. *Polymer*, in press.
(49) Flory, P. J.; Fox, T. G. *J. Am. Chem. Soc.* **1951**, *73*, 1907, 1909, 1915.
(50) Kirkwood, J. G. *J. Chem. Phys.* **1939**, *7*, 911.
(51) Ishida, Y.; Yamafuji, K. *Kolloid Z.* **1964**, *200*, 48.
(52) Berry, G. C.; Fox, T. G. *Adv. Polym. Sci.* **1974**, *16*, 1.
(53) Adachi, K.; Hirano, H. *Macromolecules* **1991**, *24*, 5365.
(54) Rouse, P. E. *J. Chem. Phys.* **1953**, *21*, 1272.
(55) De Gennes, P. G. *J. Chem. Phys.* **1971**, *55*, 572.
(56) Doi, M.; Edwards, S. F. *J. Chem. Soc., Faraday Trans. 2* **1978**, *74*, 1789, 1802, 1818.
(57) Adachi, K.; Wada, T.; Kawamoto, T.; Kotaka, T. *Macromolecules* **1995**, *28*, 3588.
(58) Adachi, K.; Itoh, S.; Nishi, I.; Kotaka, T. *Macromolecules* **1990**, *23*, 2554.
(59) Graessley, W. W. *Adv. Polym. Sci.* **1982**, *47*, 68.
(60) Ferry, J. D. *Viscoelastic Properties of Polymers*, 2nd ed.; Wiley: New York, 1970.

MA0212341